Translational Oncology
www.transonc.com

Volume 6 Number 4 August 2013 pp. 429–441 429

HSP90 Inhibitor SNX5422/2112 Targets the Dysregulated Signal and Transcription Factor Network and Malignant Phenotype of Head and Neck Squamous Cell Carcinoma[1,2]

Jay A. Friedman*,[3], Stephanie C. Wise*,[3], Michael Hu*, Chris Gouveia*, Robert Vander Broek*, Christian Freudlsperger*,†, Vishnu R. Kannabiran*, Pattatheyil Arun*, James B. Mitchell‡, Zhong Chen* and Carter Van Waes*

*Tumor Biology Section, Head and Neck Surgery Branch, National Institute on Deafness and Other Communication Disorders, National Institutes of Health, Bethesda, MD; †Department of Oral and Maxillofacial Surgery, University Hospital, Heidelberg, Germany; ‡Radiation Biology Branch, National Cancer Institute, National Institutes of Health, Bethesda, MD

Abstract

Heat shock protein 90 (HSP90) is a chaperone protein that stabilizes proteins involved in oncogenic and therapeutic resistance pathways of epithelial cancers, including head and neck squamous cell carcinomas (HNSCCs). Here, we characterized the molecular, cellular, and preclinical activity of HSP90 inhibitor SNX5422/2112 in HNSCC overexpressing HSP90. SNX2112 inhibited proliferation, induced G_2/M block, and enhanced cytotoxicity, chemosensitivity, and radiosensitivity between 25 and 250 nM *in vitro*. SNX2112 showed combinatorial activity with paclitaxel in wild-type (wt) TP53-deficient and cisplatin in mutant (mt) TP53 HNSCC lines. SNX2112 decreased expression or phosphorylation of epidermal growth factor receptor (EGFR), c-MET, v-akt murine thymoma viral oncogene homolog 1 (AKT), extracellular signal–regulated kinases (ERK) 1 and 2, inhibitor κB kinase, and signal transducer and transcription factor 3 (STAT3), corresponding downstream nuclear factor κB, activator protein-1, and STAT3 reporter genes, and target oncogenes and angiogenic cytokines. Furthermore, SNX2112 enhanced re-expression of TP53 and targets p21WAF1 and PUMA, while TP53 inhibitor Pifithrin or siRNA attenuated the antiproliferative activity of SNX2112 in wtTP53 HNSCC *in vitro*. Prodrug SNX5422 similarly down-modulated key signal targets, enhanced TP53 expression and apoptosis, and inhibited proliferation, angiogenesis, and tumorigenesis in a wtTP53-deficient HNSCC xenograft model. Thus, HSP90 inhibitor SNX5422/2112 broadly modulates multiple key nodes within the dysregulated signaling network, with corresponding effects upon the malignant phenotype. Our data support investigation of SNX5422/2112 in combination with paclitaxel, cisplatin, and radiotherapy in HNSCC with different TP53 status.

Translational Oncology (2013) 6, 429–441

Address all correspondence to: Carter Van Waes, MD, PhD or Zhong Chen, MD, PhD, National Institute on Deafness and Other Communication Disorders, National Institutes of Health, CRC Rm 4-2732 or Rm 5D55, 10 Center Dr, Bethesda, MD 20892. E-mail: vanwaesc@nidcd.nih.gov, chenz@nidcd.nih.gov

[1]This work was supported by National Institute on Deafness and Other Communication Disorders (NIDCD) intramural research program projects ZIA-DC-000073 and 000074. S.C.W., M.H., C.G., R.V.B., and V.R.K. were supported by the Medical Research Training Program, a public–private partnership jointly sponsored by the National Institutes of Health (NIH) and Pfizer Inc (through a grant to the Foundation for NIH from Pfizer Inc). Synthetic HSP90 inhibitor SNX5422 (PF-04928473) and its oral prodrug SNX2112 (PF-04929113) were provided to NIDCD and C.V.W. for research under a Material Transfer Agreement with Pfizer Inc or Esanex Inc. C.V.W. has no financial interests to disclose.

[2]This article refers to supplementary materials, which are designated by Figures W1 to W5 and are available online at www.transonc.com.

[3]Contributed equally as first authors.

Received 18 March 2013; Revised 16 May 2013; Accepted 5 June 2013

 1944-7124/13
DOI 10.1593/tlo.13292

Introduction

Biologic and small molecule inhibitors selectively targeting growth factor receptors, signal kinases, and angiogenesis factor receptors have undergone extensive preclinical and clinical studies in different cancers. Relative to the success of targeted therapy against prevalent genetic drivers in some hematologic malignancies (e.g., BCR/ABL), the clinical activity of these agents in solid tumors has often been modest or transient. Head and neck squamous cell carcinomas (HNSCCs) have been the subject for clinical or preclinical studies of several targeted agents against a few commonly activated or inactivated pathways, including epidermal growth factor receptor (EGFR; cetuximab, gefitinib, and erlotinib) [1–5], proteasome-dependent nuclear factor κB (NF-κB) activation (bortezomib) [6,7], signal transducer and transcription factor 3 (STAT3; decoy oligonucleotide) [8], and disrupted tumor suppressor TP53 (TP53 adenovirus) [9]. These agents have demonstrated significant target-specific and preclinical activity but modest clinical activity at achievable concentrations as monotherapy or in combination with conventional therapies [1–9].

Studies of the signal and transcriptional mechanisms mediating pathogenesis and resistance of HNSCC demonstrate frequent alteration and complex cross talk among multiple pathways. This includes co-activation of growth factor and cytokine receptors and their ligands [EGFR, c-MET, tumor necrosis factor–α (TNF-α), interleukin-1 (IL-1), and IL-6], intermediate signal kinases [sarcoma Rous cellular homolog (SRC), MAP or extracellular signal–regulated kinase (ERK) kinase (MEK)–ERK1/2, phosphatidylinositol 3-kinase (PI3K)–v-akt murine thymoma viral oncogene homolog 1 (AKT), and inhibitor κB kinase (IKK)], and downstream transcription factors [activator protein-1 (AP-1), NF-κB, and STAT3] that promote the malignant phenotype [3,5–8,10–12]. Additionally, dysregulation of the key tumor suppressor TP53 may result from transcriptional inactivation or mutation in HNSCC subsets, which exhibit differences in response to therapy [13–15]. Recent next-generation sequencing studies in HNSCC support the prevalence of genetic alterations affecting multiple growth factor receptors, *PIK3CA* and *PTEN* that regulate AKT, components of the NF-κB pathway, and tumor suppressor *TP53* [16,17]. Thus, it has become increasingly clear that the complex genetic and epigenetic alterations in HNSCC and other solid cancers contribute to intrinsic or acquired resistance to targeted and standard cytotoxic therapies [5,7,10–14]. Therefore, combinations or agents targeting multiple components of the dysregulated network in HNSCC and other solid cancers may have potential for broader activity [18–23].

Heat shock protein 90 (HSP90) is a molecular chaperone required for the proper folding, stabilization, and function of many proteins, including multiple overexpressed, mutated, or activated signal components and transcription factors that serve as key nodes in the network of pathways that promote cancer cell proliferation and survival [24]. The ATP-dependent conformational state of HSP90 provides a selective target for natural toxins (e.g., geldanomycins) and synthetic inhibitors. Targeted inhibition of HSP90 leads to destabilization and proteasomal degradation of a diverse array of its client proteins, conveying the potential to simultaneously modulate many signaling pathways that synergize to promote cancer progression and reduce the development of resistance seen with more selective molecular targeted agents [24–26].

Prior studies provide evidence that HSP90 activation by interferon may contribute to EGF-mediated protection against the apoptotic effects of interferon in HNSCC cells [27]. We recently showed that wild-type (wt) EGFR is stabilized by HSP90 in HNSCC [28]. Enhanced activity of HSP90 inhibitor geldanomycin is observed in HNSCC with increased HSP90 and RAS activity [29]. In addition to the ability of HSP90 inhibitors to concurrently modulate multiple key molecular targets, they can enhance standard cytotoxic modalities such as chemotherapy and radiation therapy in cancers, including HNSCC [25,26,28–31].

SNX5422 (also known as PF-04929113) is a water-soluble and orally bioavailable prodrug of SNX2112 (PF-04928473), a potent and highly selective small molecule inhibitor of HSP90 [32,33]. SNX2112 competitively binds to the N-terminal ATP pocket of HSP90 family members (HSP90α, HSP90β, Grp94, and Trap-1) and is highly potent against various cancers *in vitro* and *in vivo* [34–37]. SNX5422 has recently completed phase I testing, which defined tolerated dosages, and demonstrated prolonged disease stabilization of >150 days with various schedules in 22% to 36% of subjects with treatment-refractory cancers [38–40]. However, preclinical studies of the molecular effects on the broadly dysregulated signal and transcriptional network and therapeutic activity of 5422/SNX2112 have not been reported in HNSCC. In the present study, we examined the effects of SNX2112 and prodrug SNX5422 on the broad network of dysregulated pathways and targets and therapeutic effects alone and in combination with radiation and standard chemotherapies in preclinical models of HNSCC.

Materials and Methods

Reagents

SNX5422 is a water-soluble and orally bioavailable prodrug of SNX2112, a potent and highly selective small molecule inhibitor of HSP90 [32,33]. Both were provided initially by Pfizer Inc and subsequently by Esanex Inc. Cisplatin was obtained from APP Pharmaceuticals (Lake Zurich, IL; #100351). Paclitaxel and TP53 inhibitor Pifithrin-α were from Sigma-Aldrich Inc (St Louis, MO; #T7191; P4359).

Cell Lines and Cell Culture

Nine HNSCC cell lines (UMSCC) obtained from Dr T. E. Carey (University of Michigan, Ann Arbor, MI) were recently characterized by genotype and TP53 status [13,41,42]. Normal human epidermal keratinocytes (HEKA) were obtained commercially (Invitrogen, Carlsbad, CA). The characteristics and culture conditions for UMSCC cell lines and HEKA cells were previously described [13] (see Supplementary Methods).

Real-time Reverse Transcription–Polymerase Chain Reaction

Quantitative reverse transcription–polymerase chain reaction (RT-PCR) was performed as described [13] (see Supplementary Methods).

Western Blot

Western blot was performed with antibodies indicated as described [13] (see Supplementary Methods).

Tissue Array and Immunohistochemical Staining

A human tissue array with 20 HNSCC sections and 6 normal mucosa sections [43] was used for staining for HSP90. Immunohistochemical staining of this tissue array and a HNSCC xenograft model for HSP90 client proteins were performed as described [43,44] (see Supplementary Methods).

Cell Proliferation Assay

Cell proliferation was measured by standard 3-(4,5-dimethylthiazol-2-yl)-2,5-diphenyltetrazolium (MTT) or 2,3-bis-(2-methoxy-4-nitro-5-sulfophenyl)-2H-tetrazolium-5-carboxanalide (XTT) assay (Roche Diagnostics, Indianapolis, IN [13]; see Supplementary Methods).

Cell Cycle Analysis

DNA cell cycle distribution analysis was performed by flow cytometry as described [44] (see Supplementary Methods).

Annexin V Apoptosis Detection

UMSCC-1 cells were plated in 100-mm^2 plates and treated the following day with either 0.01% DMSO control or 50, 100, or 200 nM SNX2112. After drug treatment, cells were expanded for 48 hours, collected at 70% to 80% confluence, and stained with Annexin V–fluorescein isothiocyanate and propidium iodide according to the manufacturer's instructions (Sigma APOAF).

Transient siRNA Transfection

TP53 or pooled control siRNA was constructed by Thermo Scientific (Lafayette, CO) and transfected in UMSCC-1 using Lipofectamine RNAiMax according to the manufacturer's instructions (Invitrogen; see Supplementary Methods).

Clonogenic Radiation Survival Assay

Clonogenic assay was performed as described previously [45] and in the Supplementary Methods.

Reporter Gene Assay

NF-κB, AP-1, STAT3, IL-8, and BCL-XL reporters and assays were performed as described [22,23] (see Supplementary Methods).

Cytokine Analysis

Cell culture supernatant samples were centrifuged at 14,000 rpm (10 minutes) to clear residual cellular debris. Individual bead kits for IL-6, IL-8, and vascular endothelial growth factor (VEGF) were purchased from Biosource (Invitrogen), and multiplex assays were performed and read by Luminex, as described [46]. Each sample was assayed in triplicate, and data were presented as means ± SD.

Tumor Xenograft Studies

Immunodeficient BALB/c severe combined-immunodeficiency (SCID) mice were obtained from the Frederick Cancer Research and Development Center, National Cancer Institute (Frederick, MD) and housed in a specific pathogen-free animal facility. Animal care and HSP90 inhibitor studies were performed under National Institutes of Health (NIH) Animal Care and Use Committee–approved Protocol 1102-07. Tumor xenografts were established by injecting 5×10^6 UMSCC-1 cells subcutaneously into the left flank. Tumor-bearing animals were randomized into experimental groups indicated (n = 10 each). PF-04929113 suspended in 0.5% carbomethylcellulose/0.5% Tween 80 was administered through oral gavage. Tumor size was measured three times weekly, and tumor volumes were calculated as V (cm^3) = $(L \times W^2)/2$. Tumors were harvested for immunohistochemical analysis for selected HSP90 client proteins, proliferation (Ki-67), apoptosis (terminal deoxynucleotidyl transferase nick end labeling (TUNEL)], and microvessel density (CD31) [5,7], as described in the Supplementary Methods.

Statistical Analysis

Significance of comparisons was determined where indicated by Fisher's Exact or Student's t test where indicated.

Results

SNX2112 Inhibits Proliferation, Cell Cycle and Survival of HNSCC Cells In Vitro

Detection of HSP90 has previously been reported in oral HNSCC [47]. We showed that HSP90 immunostaining was detected or increased in a majority (18 of 20) of HNSCC tumors from different anatomic sites in a tissue microarray (Figure W1, *A* and *B*). Similarly, increased expression of HSP90 mRNA and protein was detected by RT-PCR and by Western blot in nine of nine HNSCC (UMSCC) cell lines compared to human keratinocytes (Figure W1, *C*–*E*). The panel included UMSCC lines derived from patients with aggressive HNSCC (survival < 15 months), and exhibiting underexpression of wtTP53 (UMSCC-1, -6, -9) or overexpression of mutant (mt) TP53 (UMSCC-11A, -11B, -22B, -38, -46) [13,42]. Thus, the pattern of increased expression of HSP90 in tumor tissue specimens and cell lines supports the rationale for investigation of the molecular, cellular, and antitumor activity of HSP90 inhibitors in HNSCC models.

Next, the effect of selective HSP90 ATPase inhibitor SNX2112 [32,33] on proliferation of a subpanel of six of these UMSCC lines was examined over 5 days by MTT assay (Figures 1*A* and W2). SNX2112 inhibited cell density in a dose-dependent manner with an inhibitory concentration 50% (IC_{50}) range of 22 to 68 nM (Figure 1*A*), demonstrating activity over a similar range in six distinct UMSCC cell lines, without apparent relationship to HSP90 overexpression (Figure W1) or TP53 genotype. Cell cycle and cytotoxic effects of SNX2112 HSP90 inhibition were further examined by propidium iodide DNA flow cytofluorometric analysis and compared in UMSCC-1 (wtTP53) and UMSCC-38 (mtTP53) cells (Figures 1*B*, *left panels*, and W3). In wtTP53 UMSCC-1, SNX2112 at 50 nM inhibited cell cycle, with increased accumulation in the G_2/M phase compared to untreated controls, 49% *versus* 23% at 48 hours (Figure 1*B*, *left panels*) and 29% *versus* 17% at 72 hours (not shown). There was also increased accumulation of fragmented sub-G_0 DNA (15%) compared to untreated controls (1%) at 48 hours (Figure 1*B*, *left panels*) and 28% *versus* 2%, respectively, at 72 hours (not shown), indicative of cell death. We performed Annexin V–fluorescein isothiocyanate staining, providing evidence for increased apoptosis with concentration (Figure 1*B*, *right panels*). Treatment of mtTP53 UMSCC-38 cells with 50 nM SNX2112 for 48 hours showed a similar accumulation in the G_2/M phase (48% *vs* 18%) but a lesser increase in sub-G_0 cells (6% *vs* 4%; Figure W3), consistent with the higher IC_{50} observed in Figure 1*A*. This trend was also seen after 72 hours of drug treatment. The results suggested that despite similarities in G_2/M cell cycle block, the UMSCC-1 line deficient for wt TP53 and lower IC_{50} was more sensitive to apoptosis than the UMSCC-38 line with mtTP53 and highest IC_{50}. To examine the potential contribution of wtTP53 in UMSCC-1 to antiproliferative effects of SNX2112, cells were pretreated with TP53 inhibitor Pifithrin or TP53 siRNA before SNX2112. Pifithrin and TP53 siRNA attenuated the antiproliferative

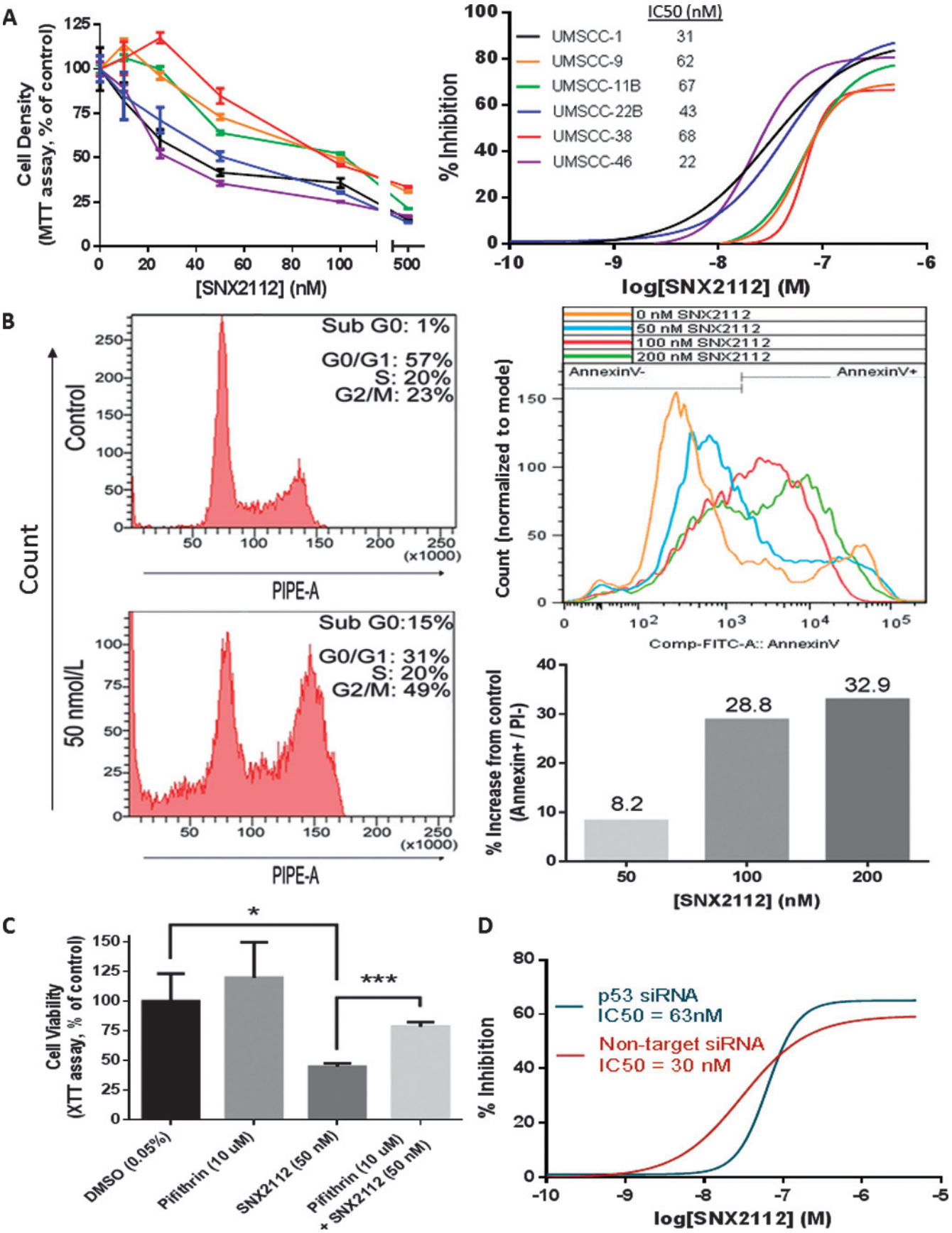
A
Cell Density (MTT assay, % of control)
[SNX2112] (nM)
IC50 (nM)
UMSCC-1 31
UMSCC-9 62
UMSCC-11B 67
UMSCC-22B 43
UMSCC-38 68
UMSCC-46 22
% Inhibition
log[SNX2112] (M)
B
Count
Control
Sub G0: 1%
G0/G1: 57%
S: 20%
G2/M: 23%
PIPE-A
50 nmol/L
Sub G0:15%
G0/G1: 31%
S: 20%
G2/M: 49%
0 nM SNX2112
50 nM SNX2112
100 nM SNX2112
200 nM SNX2112
AnnexinV-
AnnexinV+
Count (normalized to mode)
Comp-FITC-A:: AnnexinV
% Increase from control (Annexin+ / PI-)
8.2
28.9
32.9
[SNX2112] (nM)
C
Cell Viability (XTT assay, % of control)
DMSO (0.05%)
Pifithrin (10 uM)
SNX2112 (50 nM)
Pifithrin (10 uM) + SNX2112 (50 nM)
D
p53 siRNA IC50 = 63nM
Non-target siRNA IC50 = 30 nM
% Inhibition
log[SNX2112] (M)

effects and doubled the IC_{50} of SNX2112, supporting a role for wtTP53 in effects of the HSP90 inhibitor in UMSCC-1 (Figure 1, *C* and *D*).

SNX2112 Inhibits Cell Survival and Sensitizes HNSCC Tumor Cells to γ-Radiation and Chemotherapy In Vitro

The observed effects of SNX2112 on sub-G_0 cell death as well as G_2/M phases of the cell cycle sensitive to radiation, led us to further investigate the effects of HSP90 inhibition on clonogenic cell survival without and with radiation in UMSCC-1 *in vitro*. While MTT assay indicated the IC_{50} for proliferation of UMSCC-1 was ~30 nM, pilot clonogenic survival assays with SNX2112 alone indicated that inhibitory concentrations for clonogenic cell survival were in a higher range, between 100 nM (90% survival) and 500 nM (59% survival), consistent with the relatively modest effects of the lower concentration of HSP90 inhibitor on cell survival seen by DNA flow cytometry. Pre-exposure of cells to an intermediate concentration of SNX2112 of 250 nM alone for 24 hours had a modest effect on clonogenic tumor cell survival [surviving fraction of 73.5 ± 9.5% (SD)], but this concentration significantly enhanced radiosensitivity, with a dose modification factor (DMF) of 1.55 ± 0.11 (fold ± SD) at 10% survival (Figure 2*A*). Post-radiation treatment for 24 hours with 250 nM SNX2112 showed no enhancement of radiosensitivity (data not shown).

We next examined the combinatorial effects of HSP90 inhibitor with chemotherapeutic agents paclitaxel and cisplatin, which are active in HNSCC, using two wtTP53 and two mtTP53 UMSCC lines, at subtherapeutic inhibitory concentrations of SNX2112 or chemotherapy drugs alone (Figure 2*B*). Interestingly, HSP90 inhibitor and paclitaxel showed combined activity in UMSCC-1 and UMSCC-9 deficient for wtTP53, while combined activity with cisplatin was observed in cell lines UMSCC-38 and UMSCC-46 expressing mtTP53. Conversely, sensitization to paclitaxel was not observed in UMSCC-38 and UMSCC-46, or to cisplatin in UMSCC-1 or UMSCC-9 (data not shown), indicating that response to these chemotherapy drugs in combination with HSP90 inhibitor was associated with differences in TP53 status. Together, the above results indicate that HSP90 inhibition has antiproliferative, cytotoxic, radiation, and chemosensitizing activity, associated with TP53 genotype in HNSCC lines *in vitro*. The SNX2112 concentrations of 22 to 68 nM having antiproliferative and chemosensitizing activity in MTT assay, and 250 nM having radiosensitizing activity in clonogenic assay, are clinically relevant, as they are within the range of concentration maxima achievable (C_{max}~77-4098 nM) in patient serum between dosages of 4 and 133 mg/m^2, where disease stabilization was observed in a recent NIH phase I clinical trial [38].

SNX2112 Inhibits Oncogenic Signaling Pathways and Induces TP53 Protein and Target Gene Expression In Vitro

Western blot analysis of UMSCC-1 (deficient wtTP53) and UMSCC-38 (mtTP53) cells treated over a range of inhibitory concentrations of SNX2112 revealed modulation of expression of several important signaling molecules, transcription factors, and target genes previously shown to be altered and promote the malignant phenotype of HNSCC (Figures 3 and W4). Lower SNX2112 concentrations of 25 to 50 nM tested initially inhibited expression of hepatocyte growth factor (HGF) receptor c-MET and phosphorylation of downstream kinases AKT (Ser^{473} and Thr^{308}) and ERK1/2 in both cell lines (Figures 3*A* and W4, *left panels*). AKT phosphorylation exhibited an oscillatory pattern of inhibition and reactivation between 24 and 72 hours in both lines, similar to that observed with PI3K-mTOR inhibitors, as reported with loss of mTOR-mediated negative feedback inhibition of PI3K [48]. Higher concentrations of 100 to 200 nM for 24 to 72 hours were required for decrease of growth factor receptor EGFR, prosurvival pathway components phospho-STAT3 and total STAT3, IKKα and β, phospho–NF-κB/p65, NF-κB– and STAT3–co-regulated prosurvival protein BCL-XL, and cleavage of cell death marker poly (ADP-ribose) polymerase (c-PARP Figures 3*A* and W4, *right panels*). Further examination of the SNX2112-sensitive UMSCC-1 line deficient for wtTP53 revealed that the inhibitor also upmodulated expression of TP53 and its target proteins, p21WAF1 and isoform PUMAα, in a time- and dose-dependent manner over 72 hours (Figure 3*A*, *left panels*). SNX2112 also enhanced expression of p21WAF1 in UMSCC-38 (Figure W4), previously shown to overexpress a missense mtTP53 and TAp73, which can also potentially activate TP53 target genes [13].

We further assessed the functional effects of HSP90 inhibitor on reporter activity for downstream proto-oncogenic transcription factors and expression of several of their target genes and proteins implicated in phenotype and resistance of HNSCC. Overall, SNX2112 significantly inhibited NF-κB, AP-1, and STAT3-specific reporter genes (Figure 3*B*) over a concentration range within which inhibition of known upstream signal molecules was observed above. However, weaker inhibition of STAT3 reporter activity was detected

Figure 1. Effect of SNX2112 on cell density, cell cycle, survival, and dependence on TP53 *in vitro*. (A) Left panel: Cellular density by MTT-based colorimetric assay for UMSCC-1 cells after 3 days of drug treatment. Right panel: IC_{50} values for six UMSCC cell lines for day 3 of drug treatment from cellular density MTT-based colorimetric assays. Cell lines treated with five drug concentrations indicate dose-dependent inhibition of cellular proliferation with IC_{50} values between 22 nM for UMSCC-46 and 68 nM for UMSCC-38. (B) Left panel: Flow cytometric cell cycle analysis using propidium iodide DNA staining of UMSCC-1 cells following 48 hours of treatment with 50 nM SNX2112. Drug treatment led to accumulation of cells in the sub-G_0 and G_2/M phases compared to controls. Right panel: Apoptosis marker Annexin V+/PI− staining after 48 hours of treatment with 50, 100, or 200 nM SNX2112 compared to DMSO control. (C) wtTP53 UMSCC-1 was pretreated for 5 hours with 10 μM Pifithrin-α, a selective inhibitor of TP53, or DMSO control and subsequently exposed to 50 nM SNX2112 or DMSO control for 2 days. Cell density was measured through XTT assay 2 days after drug exposure. Pifithrin-α treatment alone did not inhibit growth of UMSCC-1. Combination treatment of UMSCC-1 with Pifithrin-α and SNX2112 attenuates the inhibitory effects of SNX2112 alone. Statistical analysis was performed using a Student's *t* test with $*P \leq .01$ and $***P \leq .001$. (D) wtTP53 UMSCC-1 cells were simultaneously transfected with p53-targeting siRNA or nontargeting control siRNA and, the following day, were treated with a range of SNX2112 doses from 1 nM to 5 μM. Two days after drug exposure, IC_{50} of each condition was determined using a nonlinear regression model.

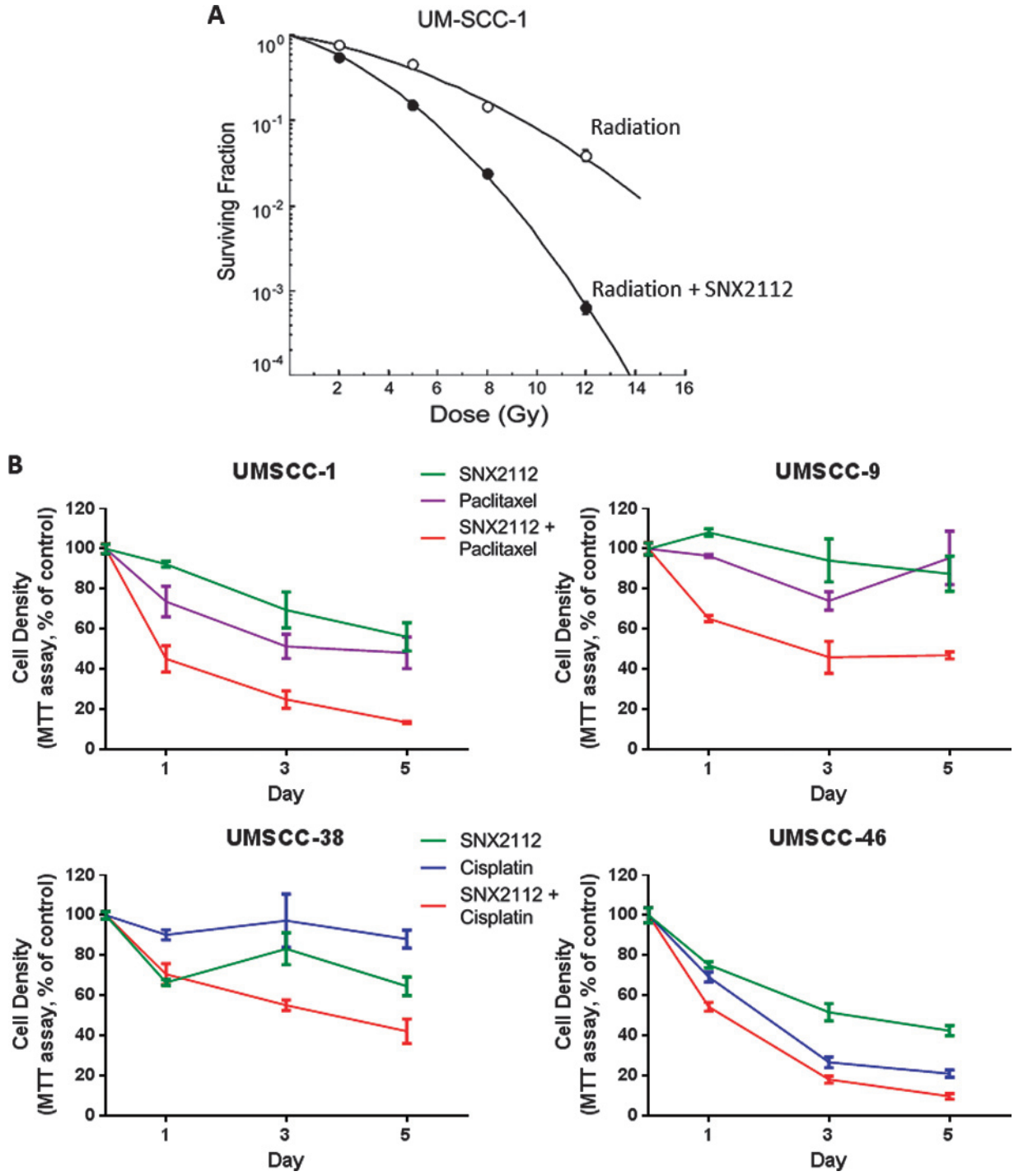

Figure 2. Effect of SNX2112 in combination with radiotherapy or chemotherapy. (A) Clonogenic survival curves for UMSCC-1 cells treated with radiation alone (open circles) or 250 nM SNX2112 for 24 hours followed by radiation (closed circles). The DMF was 1.55 ± 0.11, revealing a radiosensitizing drug effect. (B) Two HNSCCs with wtTP53 (UMSCC-1 and UMSCC-9) and two with mtTP53 genotype (UMSCC-38 and UMSCC-46) were incubated with paclitaxel, cisplatin, and SNX2112 alone or in combination at subinhibitory concentrations for the drugs for the cell lines. These were given as follows: 25 nM SNX2112 and 3 nM paclitaxel for UMSCC-1; 37.5 nM SNX2112 and 3 nM paclitaxel for UMSCC-9; 75 nM SNX2112 and 10 μM cisplatin for UMSCC-38, and 37.5 nM SNX2112 and 2.5 μM cisplatin for UMSCC-46. SNX2112 showed combinatorial activity with paclitaxel in HNSCC with wtTP53 (UMSCC-1 and UMSCC-9) and with cisplatin in lines with mtTP53 (UMSCC-38 and UMSCC-46) by MTT assay.

beginning at lower concentrations than required for inhibition of STAT3 phosphorylation and incompletely inhibited at higher concentrations where minimal STAT3 phosphorylation was detected at 48 hours in Figure 3*A*, suggesting the drug may have more complex effects involving other determinants of STAT activation or STAT family members. IL-8 cytokine and BCL-XL prosurvival gene reporters sharing enhancer elements for two or three of these transcription factors were also inhibited (Figure 3*B*). Furthermore, SNX2112

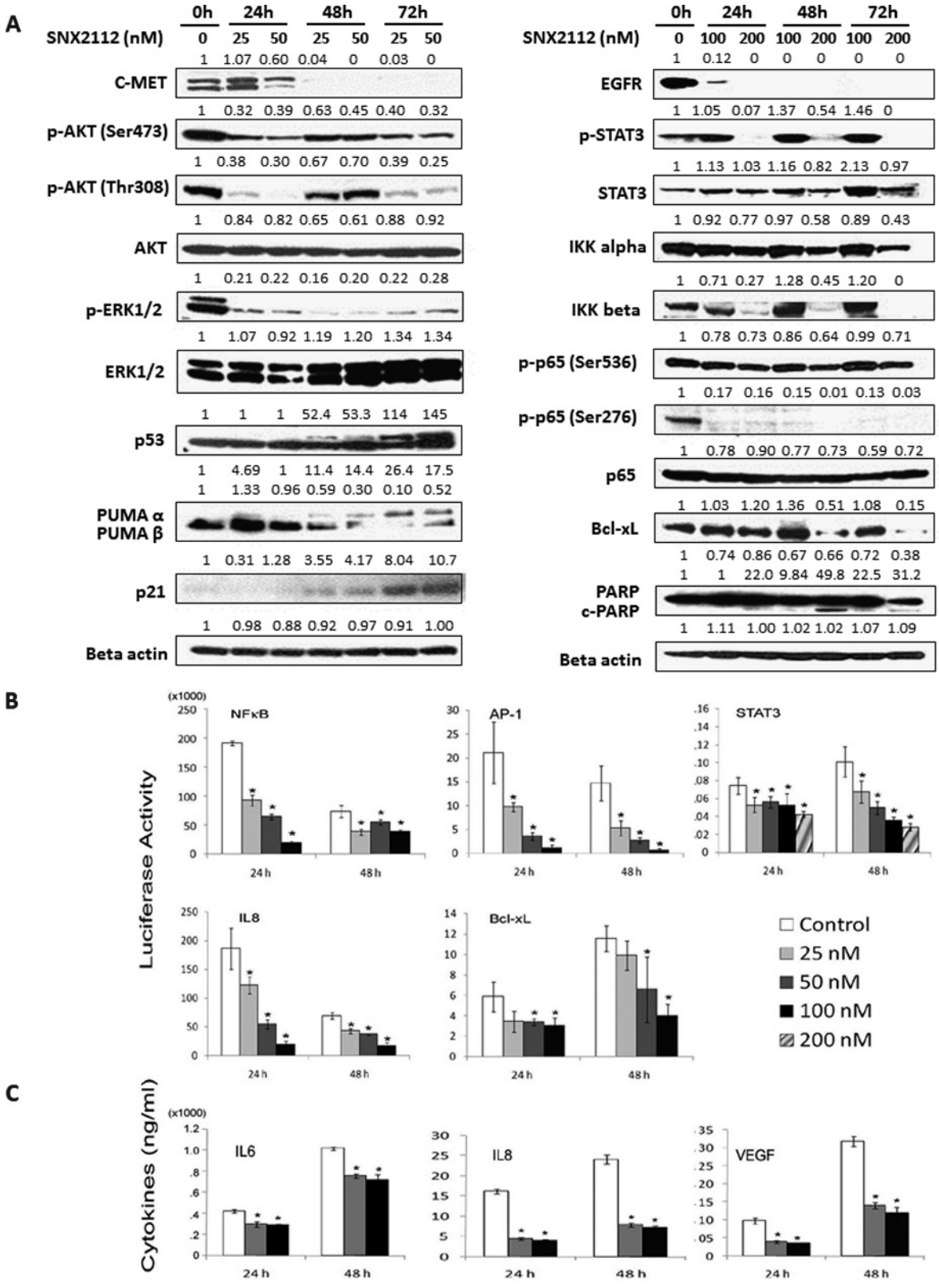

Figure 3. Effects of SNX2112 on oncogenic HSP90 clients, TP53 and target protein expression, prosurvival transcription factors, and proinflammatory and angiogenic cytokines *in vitro*. (A) Western blot analysis of whole-cell lysates from UMSCC-1 cells treated with 25 or 50 nM SNX2112 (left panel) or 100 or 200 nM SNX2112 (right panel) for 24, 48, and 72 hours. Protein density relative to 0-hour untreated control and actin loading control is quantified above each individual protein band. (B) Reporter gene activity of plasmid-transfected tumor cells in the presence of SNX2112 at 24 and 48 hours. Reporter plasmids include NF-κB, AP-1, STAT3, IL-8, and BCL-XL. *$P < .05$ indicates statistical difference between control and SNX2112-treated groups (Student's *t* test). (C) Luminex multiplex assay measuring tumor cell production of IL-6, IL-8, and VEGF cytokines in the presence of increasing concentrations of SNX2112 at 24 and 48 hours. *$P < .05$ indicates statistically significant difference compared to controls.

inhibited expression of NF-κB– and AP-1–co-regulated IL-6, IL-8, and VEGF proteins implicated in tumor angiogenesis [49–52] in culture supernatants (Figure 3*C*). Consistent with inhibition of ERK and AP-1, AP-1 target VEGF was decreased by treatment with SNX2112 (50 nM). Significant inhibition of IKK–NF-κB and dependent gene *IL-8* required intermediate drug concentrations ≥100 nM. Inhibition of STAT3 inducer IL-6, STAT3, and co-regulated target BCL-XL required drug concentrations ≃200 nM. The cumulative effects of increasing concentrations of SNX2112 on key components of these signal transduction pathways and targets are consistent with the ranges in which significant inhibition of cell density in MTT assay (25-50 nM), angiogenesis factor expression (>100 nM), and decreased radiation clonogenic cell survival (250 nM) were observed.

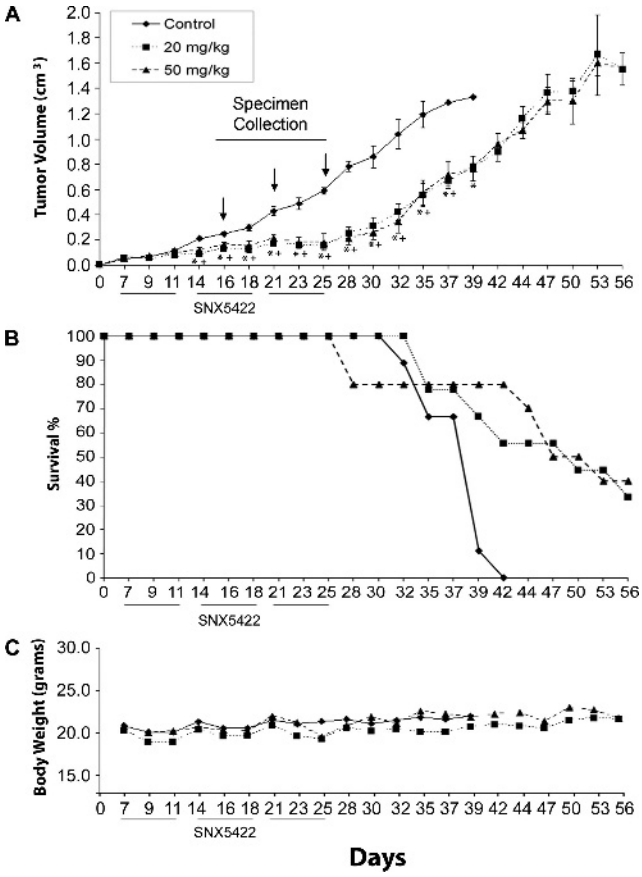

Figure 4. Effect of SNX5422 on tumor growth *in vivo*. SCID mice were inoculated on day 0 with UMSCC-1 cells, then randomized and treated on day 7. Mice received 20 mg/kg SNX5422 on a Monday to Friday daily schedule or received 50 mg/kg SNX5422 on a Monday, Wednesday, Friday schedule. Drug dissolved in methylcellulose solution or methylcellulose alone as control was given through oral gavage. Mice were treated for a total of 3 weeks (indicated by bars along the *x*-axis). (A) Tumor growth, (B) survival, and (C) body weight in control and treated animals. $^{*}P < .05$ indicates statistical difference between control and 20 mg/kg treated group (Student's *t* test); $^{+}P < .05$ indicates statistical difference between control and 50 mg/kg treated group (Student's *t* test). Arrows above tumor growth curves (A) indicate days 16, 21, and 25 when tumors were harvested from all three experimental groups for immunohistochemical analysis.

SNX5422 Inhibits Tumorigenesis and Modulates Markers of Proliferation, Apoptosis, and Angiogenesis In Vivo

We next examined the effects of the prodrug SNX5422 on tumor growth, survival, and angiogenesis and a panel of these molecular markers in wtTP53-deficient UMSCC-1 xenografts *in vivo*. After tumors were established, SNX5422 was administered for 21 days on two different dose schedules, 20 mg/kg daily (Monday to Friday) or 50 mg/kg every other day (Monday, Wednesday, and Friday). The concentration average for free drug for 50 mg/kg every other day used in mice is approximately equivalent to that achieved with 100 mg/m^2 in human phase I studies (J. Kan, N. Brega, and Pfizer, unpublished pharmacokinetic data). Biologic outcomes, including tumor growth, survival, and body weight, were measured and compared to placebo-treated controls (Figure 4). The rate of tumor growth was significantly and similarly inhibited in both 20 mg/kg (Monday to Friday) and 50 mg/kg (Monday, Wednesday, and Friday) treatment groups compared to controls while on treatment for 3 weeks. Once treatment was discontinued, both experimental groups demonstrated tumor growth at a rate similar to that seen in controls (Figure 4*A*). Suppression of tumor growth corresponded with a survival benefit for treated animals *versus* controls of ~2 weeks (Figure 4*B*). Toward the end of 3 weeks of treatment with SNX5422, 50 mg/kg (Monday, Wednesday, and Friday), gastrointestinal and systemic toxicities (diarrhea, piloerection, and lethargy) were observed and associated with death in 2 of 10 animals. The toxicities resolved in the remaining animals once the drug was discontinued. No systemic toxicity was apparent in the lower dose treatment group. A second controlled study of treatment with the lower dose of SNX5422, 20 mg/kg (5 days per week), for up to 6.5 weeks revealed sustained tumor stabilization while on treatment, an overall survival benefit exceeding 2 weeks, and minimal toxicity (Figure W5). In both studies, fluctuation in body weight was seen during weekdays of treatment in both vehicle and drug-treated mice, likely due to hyperosmotic or other effects of the methylcellulose/Tween 80 vehicle used for drug delivery.

Effects of HSP90 Inhibition on Target Biomarkers In Vivo

Tumor specimens from extra control and mice treated with both concentrations/schedules during the 3-week *in vivo* study were harvested on days 16, 21, and 25 after tumor inoculation (days 9, 14, and 18 of treatment) for immunohistochemical comparison of selected HSP90 clients characterized above and markers of proliferation (Ki-67), apoptosis (TUNEL), and angiogenesis (CD31). Maximal effects on individual tumor markers were observed in specimens by day 16 or day 21, and representative sections demonstrating treatment-induced modulation are shown in Figure 5*A*. HNSCC tumors from SNX5422-treated mice showed decreased immunostaining for pro-growth and prosurvival signal molecules c-MET, SRC, p-AKT, and p-ERK1/2 and transcription factor p-STAT3, while that for pro-apoptotic transcription factor TP53 and target PUMA was increased. Corresponding to the well-established cellular functions of these pathways, SNX5422 inhibited proliferation, as indicated by reduced Ki-67, and induced apoptosis, as evidenced by an increase in tumor apoptotic index, measured by TUNEL staining (Figure 5, *A* and *B*). Consistent with the inhibition of tumor angiogenic cytokine production observed *in vitro* (Figure 4*C*), tumors treated with SNX5422 also showed an overall reduction in CD31+ vessel density (Figure 5, *A* and *B*). Together, these results provide evidence that SNX5422 treatment suppresses tumor growth *in vivo* by modulating the expression of known clients

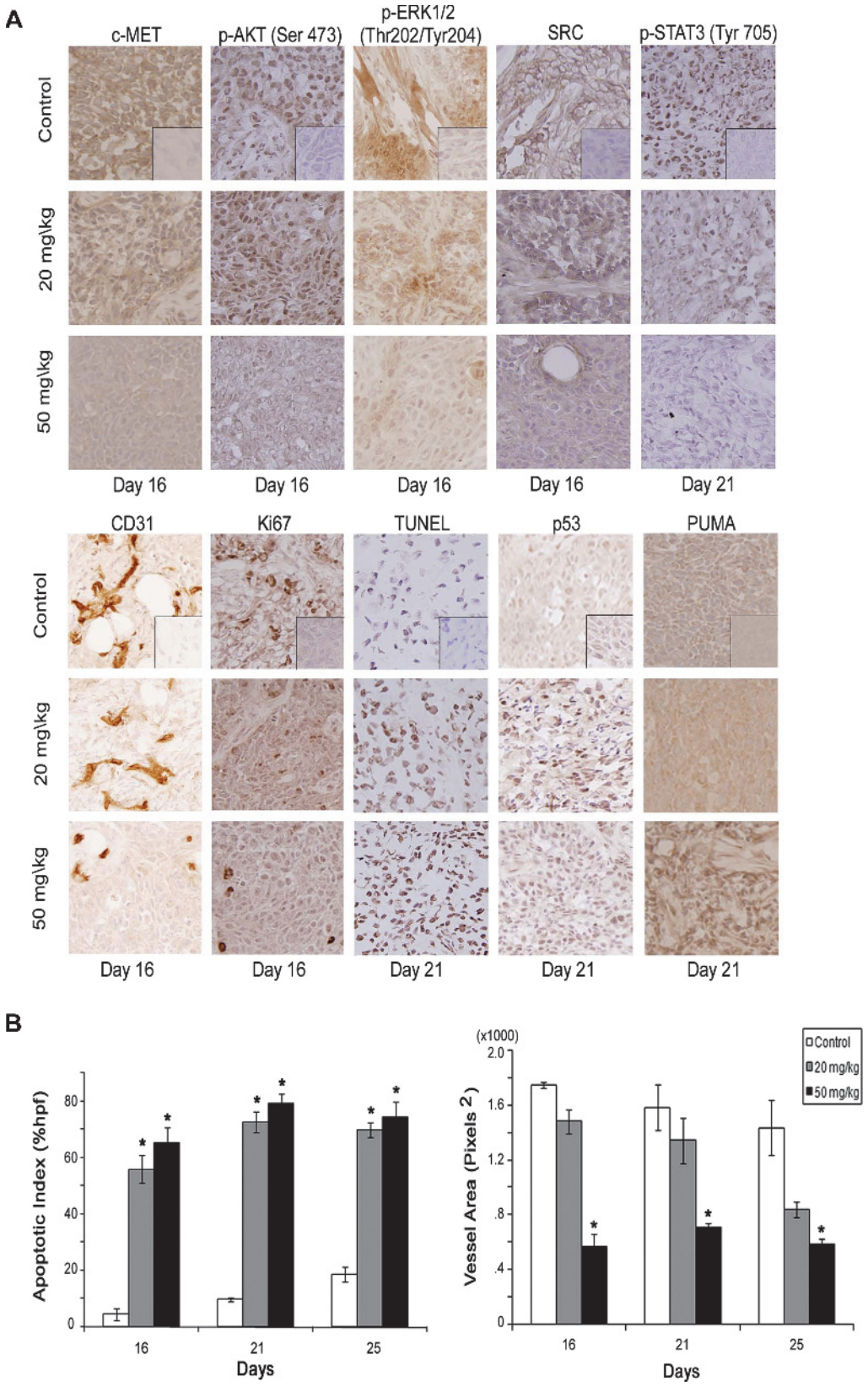

Figure 5. SNX5422 effects on molecular markers *in vivo*. Tumors were harvested from control and treated mice on days 16, 21, and 25, and frozen sections were prepared for immunohistochemical analysis of tumor marker expression. Maximal effects of drug-induced modulation of individual tumor marker expression were observed on day 16 or day 21, and representative sections are shown. (A) Immunostaining patterns of c-MET, p-AKT, p-ERK1/2, SRC, and p-STAT3 (top panel) as well as CD31, Ki-67, TUNEL, p53, and PUMA (bottom panel) were compared in control and treated groups (original magnification, ×400). (B) TUNEL assay was performed to quantify apoptotic cells in treated tumor specimens by counting the positive cells in three high power fields (HPFs; ×400, left panel); quantitation of CD31-positive vessel density in tumors (right panel). *$P < .05$ indicates statistical difference between treated groups and controls (Student's *t* test).

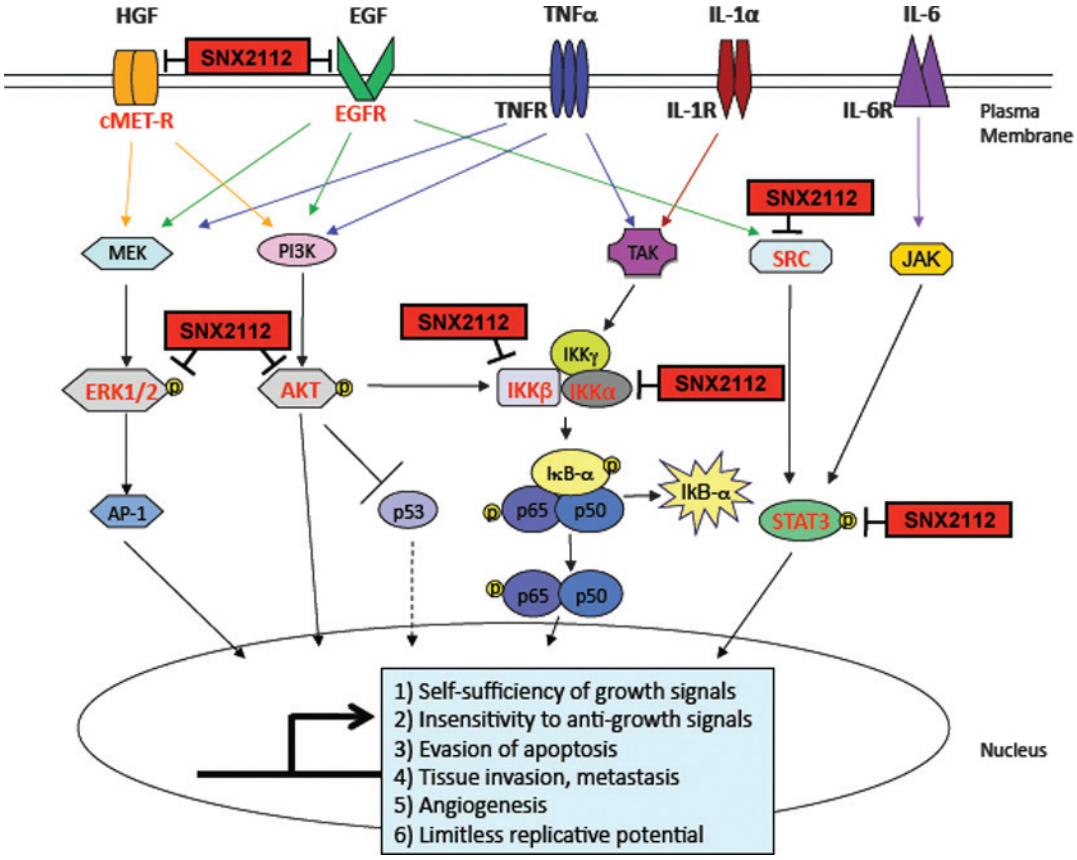

Figure 6. Model of the signal transduction and transcription factor network in HNSCC. Key components of the signal transduction and transcription factors implicated in cell proliferation, survival, and malignant phenotype of HNSCC are shown. Labels in red depict HSP90 clients forming key nodes that are inhibited by SNX5422/2112 (see Discussion section for details). Abbreviations: HGF/c-MET-R, hepatocyte growth factor/c-MET receptor; EGF/EGFR, epidermal growth factor/receptor; TNF-α/TNFR, tumor necrosis factor–α/receptor; IL-1α/IL-1R, interleukin-1α/receptor; IL-6/IL-6R, interleukin-6/receptor; MEK, ERK kinase; ERK, extracellular signal–regulated kinase; AP-1, activator protein-1; PI3K, phosphatidylinositol 3-kinase; AKT, v-akt murine thymoma viral oncogene homolog 1; p53, protein 53 kDa; TAK, transforming growth factor β–activated kinase; IKK, inhibitor κB kinase; IκB-α, inhibitor κB B-alpha; NF-κB p65/p50, nuclear factor κB 65/50 kDa; SRC, sarcoma Rous cellular homolog; JAK, Janus activated kinase; STAT3, signal transducer and transcription factor 3.

of HSP90 and their targets mediating proliferation, survival, and angiogenesis in HNSCC.

Discussion

Here, we show that HSP90 inhibitor SNX5422/2112 inhibits proliferation of a panel of six UMSCC lines (Figure 1) that exhibit increased HSP90 (Figure W1), along with dysregulation of a network of prooncogenic signal components and tumor suppressor TP53 found in HNSCC (Figures 3, 5, and 6). HSP90 inhibition increased G_2/M cell cycle blockade, sub-G_0 DNA, and apoptotic marker Annexin (Figures 1*B* and W3) and showed combined activity with radiation or cisplatin or paclitaxel chemotherapies active in HNSCC (Figure 2). HSP90 inhibition broadly suppressed the dysregulated network of prooncogenic signal components and transcription factors *in vitro* and *in vivo* (Figures 3, W4, 5, and 6) and prolonged progression-free survival in an HNSCC xenograft model *in vivo* (Figures 4 and W5). Inhibition of prosurvival pathway components EGFR, NF-κB, STAT3, and their antiapoptotic target BCL-XL was associated with PARP cleavage and decreased clonogenic survival *in vitro* (Figures 2*A*, 3*A*, and W4*A*). TP53 inhibition by Pifithrin or siRNA partially attenuated the inhibitory effects of SNX2112 observed in UMSCC-1 with wtTP53 (Figure 1, *C* and *D*), supporting a role for TP53. Further, SNX2112 induced sub-G_0 DNA and TUNEL activity was associated with increased TP53 and target proapoptotic protein PUMA in UMSCC-1 *in vitro* and *in vivo* (Figures 3*A* and 5). Interestingly, sensitivity to HSP90 inhibitor in combination with chemotherapy agent cisplatin or paclitaxel (Figure 2*B*) also appeared to differ with TP53 status. SNX2112 enhanced paclitaxel sensitivity of UMSCC-1 and UMSCC-9 with wtTP53 but not UMSCC-38 and UMSCC-46 with mtTP53 (Figure 2*B*; not shown). Conversely, SNX2112 showed enhanced activity with cisplatin in UMSCC-38 and UMSCC-46, with mtTP53. We observed potent suppression of tumorigenesis in an HNSCC xenograft model with inhibition of EGFR, c-MET, p-AKT, p-ERK, SRC, and p-STAT3 and, conversely, the re-expression of proapoptotic TP53 and PUMA (Figures 4 and 5). Corresponding reductions in proliferation (Ki-67) and angiogenesis (CD31) and increased apoptosis by TUNEL assay were observed. Together, these preclinical studies support further investigation of SNX5422/2112 and these molecular targets, which are implicated in sensitivity to HSP90 inhibitor alone or in combination with cytotoxic chemotherapy and radiotherapy in patients with HNSCC.

We have previously shown that HNSCC tumors and UMSCC lines exhibit concurrent activation or disruption of several signaling pathways, which contain multiple HSP90 clients important in cancer

(Figure 6). These include EGFR, c-MET, and TNF receptors and their ligands that contribute to cross-activation of the MEK–ERK–AP-1 and PI3K-AKT axes [22,49–52], TNF and IL-1 that co-activate the IKK–NF-κB axis [52,53], and EGF, IL-6, or both that can variably induce MEK- or Janus activated kinase–mediated STAT3 pathway activation [50]. Conversely, we showed that tumor suppressor TP53 is inactivated or mutated in subsets of HNSCC [13] and inversely co-modulated with these other pathways, suggesting a potential linkage [22]. The altered signaling pathways in this network have been individually shown to contribute to the promotion of cell proliferation, survival, expression of inflammatory and angiogenesis factors, and therapeutic resistance that comprise important hallmarks of cancer [13,22,44–53]. However, intrinsic and acquired resistance to therapies targeting individual components, such as EGFR, proteasome-dependent activation of NF-κB, or mutated or inactivated TP53, has been attributed to limited modulation or compensatory activation of other signal molecules and pathways in experimental studies and clinical trials [5,7,12]. The concurrent modulation of multiple signaling pathways by HSP90 inhibition uniquely differentiated its effects from previous targeted agents. Specifically, EGFR inhibitors often failed to simultaneously block AKT, ERK, and SRC kinases and downstream transcription factors NF-κB, AP-1, and STAT3 [5,12]. While proteasome inhibitor bortezomib effectively inhibited the activation of NF-κB p65, it did not inhibit other signaling molecules, such as noncanonical NF-κBs, p-ERK1/2, or STAT3 [7]. MET inhibition also affected downstream signal inhibition in only a subset of HNSCC [11]. In addition to the ability of HSP90 inhibitors to concurrently modulate multiple key molecular targets, they can enhance standard cytotoxic modalities such as chemotherapy and radiation therapy in HNSCC (Figure 2).

In our study, we observed differential activity of SNX2112 on cell growth arrest, apoptosis, combination therapy, and HSP90 client expression based on dose and duration of exposure to drug and the cell line examined. At lower concentrations (25-50 nM SNX2112), inhibition of c-MET, p-AKT, and p-ERK and induction of TP53 and p21 were associated with decreased cell proliferation in both UMSCC-1 and UMSCC-38 (Figures 1, 3, and W2–W4). These findings are consistent with our previous demonstration that HGF–c-MET contributes to activation of p-ERK and p-AKT and proliferation, which can be partially blocked by MEK or PI3K inhibition [49]. In the prior study, we further showed that HGF–c-MET induced MEK-ERK and PI3K-AKT activation contributes to co-expression of angiogenesis factors IL-8 and VEGF, which were also inhibited at lower concentrations of SNX2112 in the present study (Figure 3, *B* and *C*). However, oscillation and re-phosphorylation of ERK and AKT were observed at lower concentrations over the time course between 48 and 72 hours. Of potential relevance, higher concentrations of SNX2112 (≥200 nM) were required for inhibition of EGFR, which can co-activate ERK, AKT, as well as STAT3, and for inhibition of IKK–NF-κB pathway components. Similarly, high concentrations of SNX2112 were required for inhibition of STAT3 and NF-κB–regulated antiapoptotic gene *BCL-XL*, cleavage of apoptotic marker PARP (Figures 3 and W4), and decreased clonogenic cell survival (Figure 2*A*). wtEGFR was recently shown to be a client but a relatively resistant target for HSP90 inhibitors [28]. Both STAT3 and IKK proteins appeared to be increased at 100 nM and required 200 nM SNX2112 for inhibition. Together, these observations suggest that incomplete HSP90 or target inhibition may enhance phosphorylation of ERK and AKT and expression of STAT3 and IKKs at concentrations below those required for destabilization and degradation of these proteins. Determination of the mechanism(s) for the compensatory enhanced expression and activation of these pathways that are critical to HNSCC cell survival could potentially lead to other combinations with HSP90 inhibitors that would enhance inhibition and cytotoxicity.

A potentially important finding of this study is that TP53, PUMA, and p21 were upmodulated by HSP90 inhibition in HNSCC with wtTP53 (Figure 3*A*). AKT has been reported to be a key node inhibiting TP53 gene transactivation by phosphorylation and modulation of cofactors, CBP/p300 and MDM2 [54–57]. Recently, another role of HSP90 inhibitors in releasing HSP90-RNA polymerase complexes paused at promoters has been implicated in upregulating repressed genes including *TP53* [58]. We also observed combined effects of SNX2112 with cytotoxic chemotherapy agents paclitaxel and cisplatin that were related to TP53 status. Paclitaxel has been reported to induce p21, inhibit microtubule-dependent cell division and G_2/M block, and induce cell death enhanced by TP53 [59], potentially explaining the combined effect observed in HNSCC with wtTP53. Cisplatin cytotoxicity can be mediated by degradation of TP53 family antagonist ΔNp63 and activation of TAp73, which we recently showed are overexpressed with mtTP53 in the subset of UMSCC that were sensitive to combined cisplatin and SNX2112 [60,61]. Confirmation of these combined effects in wider subsets could potentially help in enhancing the limited cytotoxicity observed with these chemotherapeutics and in selecting optimal combinations for patient therapy.

HSP90 inhibition potently suppressed tumorigenesis in a preclinical HNSCC xenograft model in concert with potent inhibition of prooncogenic signaling and induction of expression of proapoptotic TP53. Supporting the clinical potential of HSP90 inhibition and SNX5422, a recent NIH phase I study found SNX5422 administered twice weekly was well tolerated with mild adverse events [38]. Fifteen of 32 patients (47%) achieved disease stabilization, with 22% exceeding 150 days after progression of a variety of treatment refractory solid tumors and lymphomas. SNX5422 administered every other day at doses ranging from 9 to 100 mg/m^2 was also tolerated, with one complete response, one partial response, and seven patients with stable disease for >150 days [35]. Diarrhea was dose limiting, as found in our murine study. However, subjects receiving 50 to 89 mg/m^2 SNX5422 daily exhibited dose-limiting ocular toxicity, and thus, every other day schedules have been recommended for future studies [39,40]. Importantly, the molecular and anticancer effects observed in HNSCC in the 25 to 250 nM range *in vitro* and concentration average for free drug for 50 mg/kg every other day used in mice in our preclinical studies were within the range attained in serum in patients who demonstrated disease-stabilizing activity and acceptable toxicity.

Regarding clinical potential of HSP90 inhibitors in squamous cell carcinoma, we previously observed prolonged stabilization of pulmonary metastasis for 8 months in a heavily pretreated patient in an NIH phase I study using geldanomycin 17-DMAG [62]. Geldanomycin derivative IPI-504 in combination with docetaxel was reported to induce partial responses or prolonged stable disease, particularly in patients with squamous cell carcinomas of the lung [63]. Together, these clinical data and our preclinical data support further investigation of SNX5422 and HSP90 inhibitors in combination with chemotherapy or radiation therapy in HNSCC.

Acknowledgments

Technical advice of J. Kan and N. Brega of Pfizer Inc and Steve Hall and Eric Orlemans of Esanex Inc are gratefully acknowledged. The authors thank Ning T. Yeh, Xinping Yang (National Institute on

Deafness and Other Communication Disorders, National Institutes of Health), and Chris Silvin (National Human Genome Research Institute, National Institutes of Health) for their technical assistance and Shivaani Kummar and Barbara Conley (National Cancer Institute, National Institutes of Health) for reading and providing helpful comments on the manuscript.

References

[1] Bonner JA, Harari PM, Giralt J, Azarnia N, Shin DM, Cohen RB, Jones CU, Sur R, Raben D, Jassem J, et al. (2006). Radiotherapy plus cetuximab for squamous-cell carcinoma of the head and neck. *N Engl J Med* **354**, 567–578.

[2] Vermorken JB, Mesia R, Rivera F, Remenar E, Kawecki A, Rottey S, Erfan J, Zabolotnyy D, Kienzer HR, Cupissol D, et al. (2008). Platinum-based chemotherapy plus cetuximab in head and neck cancer. *N Engl J Med* **359**, 1116–1127.

[3] Egloff AM and Grandis JR (2008). Targeting epidermal growth factor receptor and SRC pathways in head and neck cancer. *Semin Oncol* **35**, 286–297.

[4] Cohen EE, Halpern AB, Kasza K, Kocherginsky M, Williams R, and Vokes EE (2009). Factors associated with clinical benefit from epidermal growth factor receptor inhibitors in recurrent and metastatic squamous cell carcinoma of the head and neck. *Oral Oncol* **45**, e155–e160.

[5] Van Waes C, Allen CT, Citrin D, Gius D, Colevas AD, Harold NA, Rudy S, Nottingham L, Muir C, Chen Z, et al. (2010). Molecular and clinical responses in a pilot study of gefitinib with paclitaxel and radiation in locally advanced head-and-neck cancer. *Int J Radiat Oncol Biol Phys* **77**, 447–454.

[6] Van Waes C, Chang AA, Lebowitz PF, Druzgal CH, Chen Z, Elsayed YA, Sunwoo JB, Rudy SF, Morris JC, Mitchell JB, et al. (2005). Inhibition of nuclear factor-κB and target genes during combined therapy with proteasome inhibitor bortezomib and reirradiation in patients with recurrent head-and-neck squamous cell carcinoma. *Int J Radiat Oncol Biol Phys* **63**, 1400–1412.

[7] Allen C, Saigal K, Nottingham L, Arun P, Chen Z, and Van Waes C (2008). Bortezomib-induced apoptosis with limited clinical response is accompanied by inhibition of canonical but not alternative nuclear factor-κB subunits in head and neck cancer. *Clin Cancer Res* **14**, 4175–4185.

[8] Sen M, Thomas SM, Kim S, Yeh JI, Ferris RL, Johnson JT, Duvvuri U, Lee J, Sahu N, Joyce S, et al. (2012). First-in-human trial of a STAT3 decoy oligonucleotide in head and neck tumors: implications for cancer therapy. *Cancer Discov* **2**, 694–705.

[9] Clayman GL (2000). The current status of gene therapy. *Semin Oncol* **27**, 39–43.

[10] Wang F, Arun P, Friedman J, Chen Z, and Van Waes C (2009). Current and potential inflammation targeted therapies in head and neck cancer. *Curr Opin Pharmacol* **9**, 389–395.

[11] Seiwert TY, Jagadeeswaran R, Faoro L, Janamanchi V, Nallasura V, El Dinali M, Yala S, Kanteti R, Cohen EE, Lingen MW, et al. (2009). The MET receptor tyrosine kinase is a potential novel therapeutic target for head and neck squamous cell carcinoma. *Cancer Res* **69**, 3021–3031.

[12] Pernas FG, Allen CT, Winters ME, Yan B, Friedman J, Dabir B, Saigal K, Mundinger GS, Xu X, Morris JC, et al. (2009). Proteomic signatures of epidermal growth factor receptor and survival signal pathways correspond to gefitinib sensitivity in head and neck cancer. *Clin Cancer Res* **15**, 2361–2372.

[13] Friedman J, Nottingham L, Duggal P, Pernas FG, Yan B, Yang XP, Chen Z, and Van Waes C (2007). Deficient TP53 expression, function, and cisplatin sensitivity are restored by quinacrine in head and neck cancer. *Clin Cancer Res* **13**, 6568–6578.

[14] Bradford CR, Zhu S, Ogawa H, Ogawa T, Ubell M, Narayan A, Johnson G, Wolf GT, Fisher SG, and Carey TE (2003). P53 mutation correlates with cisplatin sensitivity in head and neck squamous cell carcinoma lines. *Head Neck* **25**, 654–661.

[15] Poeta ML, Manola J, Goldwasser MA, Forastiere A, Benoit N, Califano JA, Ridge JA, Goodwin J, Kenady D, Saunders J, et al. (2007). *TP53* mutations and survival in squamous-cell carcinoma of the head and neck. *N Engl J Med* **357**, 2552–2561.

[16] Stransky N, Egloff AM, Tward AD, Kostic AD, Cibulskis K, Sivachenko A, Kryukov GV, Lawrence MS, Sougnez C, McKenna A, et al. (2011). The mutational landscape of head and neck squamous cell carcinoma. *Science* **333**, 1157–1160.

[17] Grandis JR, Hayes DN, and El-aggar A, and The Cancer Genome Atlas Group (2012). Comprehensive genomic characterization of squamous cell carcinoma of the head and neck. In *TCGA 2nd Annual Scientific Symposium.* p. 32.

[18] Boehm AL, Sen M, Seethala R, Goodling WE, Freilino M, Wong SM, Wang S, Johnson DE, and Grandis JR (2008). Combined targeting of epidermal growth factor receptor, signal transducer and activator of transcription-3, and Bcl-X_L enhances antitumor effects in squamous cell carcinoma of the head and neck. *Mol Pharmacol* **73**, 1632–1642.

[19] Benavente S, Huang S, Armstrong EA, Chi A, Hsu KT, Wheeler DL, and Harari PM (2009). Establishment and characterization of a model of acquired resistance to epidermal growth factor receptor targeting agents in human cancer cells. *Clin Cancer Res* **15**, 1585–1592.

[20] Perrone F, Lampis A, Orsenigo M, Di Bartolomeo M, Gevorgyan A, Losa M, Frattini M, Riva C, Andreola S, Bajetta E, et al. (2009). PI3KCA/PTEN deregulation contributes to impaired responses to cetuximab in metastatic colorectal cancer patients. *Ann Oncol* **20**, 84–90.

[21] Tortora G, Ciardiello F, and Gasparini G (2008). Combined targeting of EGFR-dependent and VEGF-dependent pathways: rationale, preclinical studies and clinical applications. *Nat Clin Pract Oncol* **5**, 521–530.

[22] Lee TL, Yeh J, Friedman J, Yan B, Yang X, Yeh NT, Van Waes C, and Chen Z (2008). A signal network involving coactivated NF-κB and STAT3 and altered p53 modulates BAX/BCL-XL expression and promotes cell survival of head and neck squamous cell carcinomas. *Int J Cancer* **122**, 1987–1998.

[23] Chen Z, Ricker JL, Malhotra PS, Nottingham L, Bagain L, Lee TL, Yeh NT, and Van Waes C (2008). Differential bortezomib sensitivity in head and neck cancer lines corresponds to proteasome, nuclear factor-κB and activator protein-1 related mechanisms. *Mol Cancer Ther* **7**, 1949–1960.

[24] Miyata Y, Nakamoto H, and Neckers L (2013). The therapeutic target Hsp90 and cancer hallmarks. *Curr Pharm Des* **19**, 347–365.

[25] Zhang H and Burrows F (2004). Targeting multiple signal transduction pathways through inhibition of Hsp90. *J Mol Med* **82**, 488–499.

[26] Trepel J, Mollapour M, Giaccone G, and Neckers L (2010). Targeting the dynamic HSP90 complex in cancer. *Nat Rev Cancer* **10**, 537–549.

[27] Caraglia M, Abbruzze A, Leardi A, Pepe S, Budillon A, Baldassare G, Selleri C, Lorenzo SD, Fabbrocini A, Giuberti G, et al. (1999). Interferon-α induces apoptosis in human KB cells through a stress-dependent mitogen activated protein kinase pathway that is antagonized by epidermal growth factor. *Cell Death Differ* **6**, 773–780.

[28] Nyati MK, Ramanand SG, Whitehead C, Hiniker SM, Rehemtulla A, Pratt WB, Gouveia C, Truong K, Van Waes C, Ray D, et al. (2012). Wild-type EGFR is stabilized by direct interaction with HSP90 in cancer cells and tumors. *Neoplasia* **14**, 670–677.

[29] Misso G, Giuberti G, Lombardi A, Grimaldi A, Ricciardiello F, Giordano A, Tagliaferri P, Abbruzzese A, and Caraglia M (2013). Pharmacological inhibition of HSP90 and ras activity as a new strategy in the treatment of HNSCC. *J Cell Physiol* **228**, 130–141.

[30] Yin X, Zhang H, Burrows F, Zhang L, and Shores CG (2005). Potent activity of a novel dimeric heat shock protein 90 inhibitor against head and neck squamous cell carcinoma *in vitro* and *in vivo*. *Clin Cancer Res* **11**, 3889–3896.

[31] Yin X, Zhang H, Lundgren K, Wilson L, Burrows F, and Shores CG (2010). BIIB021, a novel Hsp90 inhibitor, sensitizes head and neck squamous cell carcinoma to radiotherapy. *Int J Cancer* **126**, 1216–1225.

[32] Huang KH, Veal JM, Fadden RP, Rice JW, Eaves J, Strachan JP, Barabasz AF, Foley BE, Barta TE, Ma W, et al. (2009). Discovery of novel 2-aminobenzamide inhibitors of heat shock protein 90 as potent, selective and orally active antitumor agents. *J Med Chem* **52**, 4288–4305.

[33] Fadden P, Huang KH, Veal JM, Steed PM, Barabasz AF, Foley B, Hu M, Partridge JM, Rice J, Scott A, et al. (2010). Application of chemoproteomics to drug discovery: identification of a clinical candidate targeting Hsp90. *Chem Biol* **17**, 686–694.

[34] Okawa Y, Hideshima T, Steed P, Vallet S, Hall S, Huang K, Rice J, Barabasz A, Foley B, Ikeda H, et al. (2009). SNX-2112, a selective Hsp90 inhibitor, potently inhibits tumor cell growth, angiogenesis, and osteoclastogenesis in multiple myeloma and other hematologic tumors by abrogating signaling via Akt and ERK. *Blood* **113**, 846–855.

[35] Rice JW, Veal JM, Barabasz A, Foley B, Fadden P, Scott A, Huang K, Steed P, and Hall S (2009). Targeting of multiple signaling pathways by the Hsp90 inhibitor SNX-2112 in EGFR resistance models as a single agent or in combination with erlotinib. *Oncol Res* **18**, 229–242.

[36] Chandarlapaty S, Sawai A, Ye Q, Scott A, Silinski M, Huang K, Fadden P, Partdrige J, Hall S, Steed P, et al. (2008). SNX2112, a synthetic heat shock protein 90 inhibitor, has potent antitumor activity against HER kinase–dependent cancers. *Clin Cancer Res* **14**, 240–248.

[37] Bachleitner-Hofmann T, Sun MY, Chen CT, Liska D, Zeng Z, Viale A, Olshen AB, Mittlboeck M, Christensen JG, Rosen N, et al. (2011). Antitumor activity of SNX-2112, a synthetic heat shock protein-90 inhibitor, in MET-amplified tumor cells with or without resistance to selective MET inhibition. *Clin Cancer Res* **17**, 122–133.

[38] Rajan A, Kelly RJ, Trepel JB, Kim YS, Alarcon SV, Kummar S, Gutierrez M, Crandon S, Zein WM, Jain L, et al. (2011). A phase I study of PF-04929113 (SNX-5422), an orally bioavailable heat shock protein 90 inhibitor, in patients with refractory solid tumor malignancies and lymphomas. *Clin Cancer Res* **17**, 6831–6839.

[39] Infante JR, Weiss GJ, Jones S, Tibes R, Bendell JC, Brega N, Torti V, Von Hoff DD, Buris HA, and Ramanathan R (2010). A phase I dose escalation study of the oral heat shock protein 90 inhibitor PF-04929113 (SNX5422) and its associated ocular toxicity. In *22nd EORTC-NCI-AACR Symposium on Molecular Targets and Cancer Therapeutics.* p. 375.

[40] Bauer TM, Infante JR, Ramanathan RK, Weiss GJ, Sachdev J, Burris HA, Hinson JM, and Orlemans EO (2013). Results of two phase 1 dose escalation studies of the oral heat shock protein 90 (Hsp90) inhibitor SNX-5422. *Am Soc Clin Oncol* **2013**, 117030.

[41] Brenner JC, Graham MP, Kumar B, Saunders LM, Kupfer R, Lyons RH, Bradford CR, and Carey TE (2010). Genotyping of 73 UM-SCC head and neck squamous cell carcinoma cell lines. *Head Neck* **32**, 417–426.

[42] Yan B, Yang X, Lee TL, Friedman J, Tang J, Van Waes C, and Chen Z (2007). Genome-wide identification of novel expression signatures reveal distinct patterns and prevalence of binding motifs for p53, nuclear factor-κB and other signal transcription factors in head and neck squamous cell carcinoma. *Genome Biol* **8**, R78.

[43] Lee TL, Yang XP, Yan B, Friedman J, Duggal P, Bagain L, Dong G, Yeh NT, Wang J, Zhou J, et al. (2007). A novel nuclear factor-κB gene signature is differentially expressed in head and neck squamous cell carcinomas in association with TP53 status. *Clin Cancer Res* **13**, 5680–5691.

[44] Arun P, Brown MS, Ehsanian R, Chen Z, and Van Waes C (2009). Nuclear NF-κB p65 phosphorylation at serine 276 by protein kinase A contributes to the malignant phenotype of head and neck cancer. *Clin Cancer Res* **15**, 5974–5984.

[45] Kato T, Duffey DC, Ondrey FG, Dong G, Chen Z, Cook JA, Mitchell JB, and Van Waes C (2000). Cisplatin and radiation sensitivity in human head and neck squamous carcinomas are independently modulated by glutathione and transcription factor NF-κB. *Head Neck* **22**, 748–759.

[46] Allen C, Duffy S, Teknos T, Islam M, Chen Z, Albert PS, Wolf G, and Van Waes C (2007). Nuclear factor-κB–related serum factors as longitudinal biomarkers of response and survival in advanced oropharyngeal carcinoma. *Clin Cancer Res* **13**, 3182–3190.

[47] Ito T, Kawabe R, Kurasono Y, Hara M, Kitamura H, Fujita K, and Kanisawa M (1998). Expression of heat shock proteins in squamous cell carcinoma of the tongue: an immunohistochemical study. *J Oral Pathol Med* **27**, 18–22.

[48] Freudlsperger C, Burnett JR, Friedman JA, Kannabiran VR, Chen Z, and Van Waes C (2011). EGFR-PI3K-AKT-mTOR signaling in head and neck squamous cell carcinomas: attractive targets for molecular-oriented therapy. *Expert Opin Ther Targets* **15**, 63–74.

[49] Dong G, Chen Z, Li ZY, Yeh NT, Bancroft CC, and Van Waes C (2001). Hepatocyte growth factor/scatter factor-induced activation of MEK and PI3K signal pathways contributes to expression of proangiogenic cytokines interleukin-8 and vascular endothelial growth factor in head and neck squamous cell carcinoma. *Cancer Res* **61**, 5911–5918.

[50] Lee TL, Yeh J, Van Waes C, and Chen Z (2006). Epigenetic modification of SOCS-1 differentially regulates STAT3 activation in response to interleukin-6 receptor and epidermal growth factor receptor signaling through JAK and/or MEK in head and neck squamous cell carcinomas. *Mol Cancer Ther* **5**, 8–19.

[51] Bancroft CC, Chen Z, Yeh J, Sunwoo JB, Yeh NT, Jackson S, Jackson C, and Van Waes C (2002). Effects of pharmacologic antagonists of epidermal growth factor receptor, PI3K and MEK signal kinases on NF-κB and AP-1 activation and IL-8 and VEGF expression in human head and neck squamous cell carcinoma lines. *Int J Cancer* **99**, 538–548.

[52] Bancroft CC, Chen Z, Dong G, Sunwoo JB, Yeh N, Park C, and Van Waes C (2001). Coexpression of proangiogenic factors IL-8 and VEGF by human head and neck squamous cell carcinoma involves coactivation by MEK-MAPK and IKK-NF-κB signal pathways. *Clin Cancer Res* **7**, 435–442.

[53] Wolf JS, Chen Z, Dong G, Sunwoo JB, Bancroft CC, Capo DE, Yeh NT, Mukaida N, and Van Waes C (2001). IL (interleukin)-1α promotes nuclear factor-κB and AP-1-induced IL-8 expression, cell survival, and proliferation in head and neck squamous cell carcinomas. *Clin Cancer Res* **7**, 1812–1820.

[54] Mayo LD and Donner DB (2001). A phosphatidylinositol 3-kinase/Akt pathway promotes translocation of Mdm2 from the cytoplasm to the nucleus. *Proc Natl Acad Sci USA* **98**, 11598–11603.

[55] Guo C, Gasparian AV, Zhuang Z, Bosykh DA, Komar AA, Gudkov AV, and Gurova KV (2009). 9-Aminoacridine-based anticancer drugs target the PI3K/AKT/mTOR, NF-κB and p53 pathways. *Oncogene* **28**, 1151–1161.

[56] Sasaki M, Nie L, and Maki CG (2007). MDM2 binding induces a conformational change in p53 that is opposed by heat-shock protein 90 and precedes p53 proteasomal degradation. *J Biol Chem* **282**, 14626–14634.

[57] Peng Y, Chen L, Li C, Lu W, and Chen J (2001). Inhibition of MDM2 by hsp90 contributes to mutant p53 stabilization. *J Biol Chem* **276**, 40583–40590.

[58] Sawarkar R, Sievers C, and Paro R (2012). Hsp90 globally targets paused RNA polymerase to regulate gene expression in response to environmental stimuli. *Cell* **149**, 807–818.

[59] Blagosklonny MV, Schulte TW, Nguyen P, Mimnaugh EG, Trepel J, and Neckers L (1995). Taxol induction of p21WAF1 and p53 requires c-raf-1. *Cancer Res* **55**, 4623–4626.

[60] Sen T, Chang X, Sidransky D, and Chatterjee A (2010). Regulation of ΔNp63α by NFκÂ. *Cell Cycle* **9**, 4841–4847.

[61] Lu H, Yang X, Duggal P, Allen CT, Yan B, Cohen J, Nottingham L, Romano RA, Sinha S, King KE, et al. (2011). TNF-α promotes c-REL/ΔNp63α interaction and TAp73 dissociation from key genes that mediate growth arrest and apoptosis in head and neck cancer. *Cancer Res* **71**, 6867–6877.

[62] Kummar S, Gutierrez ME, Gardner ER, Chen X, Figg WD, Zajac-Kaye M, Chen M, Steinberg SM, Muir CA, Yancey MA, et al. (2010). Phase I trial of 17-dimethylaminoethylamino-17-demethoxygeldanamycin (17-DMAG), a heat shock protein inhibitor, administered twice weekly in patients with advanced malignancies. *Eur J Cancer* **46**, 340–347.

[63] Riely GJ, Gettinger SN, Stoller RG, Gabrail NY, Dy GK, Weiss GJ, Tunkey C, Skliris G, Strychor S, Dunbar J, et al. (2011). Safety and activity of IPI-504 (retaspimycin hydrochloride) and docetaxel in pretreated patients with metastatic non-small cell lung cancer (NSCLC). *J Clin Oncol* **29**, 2011(suppl; abstr 7516).

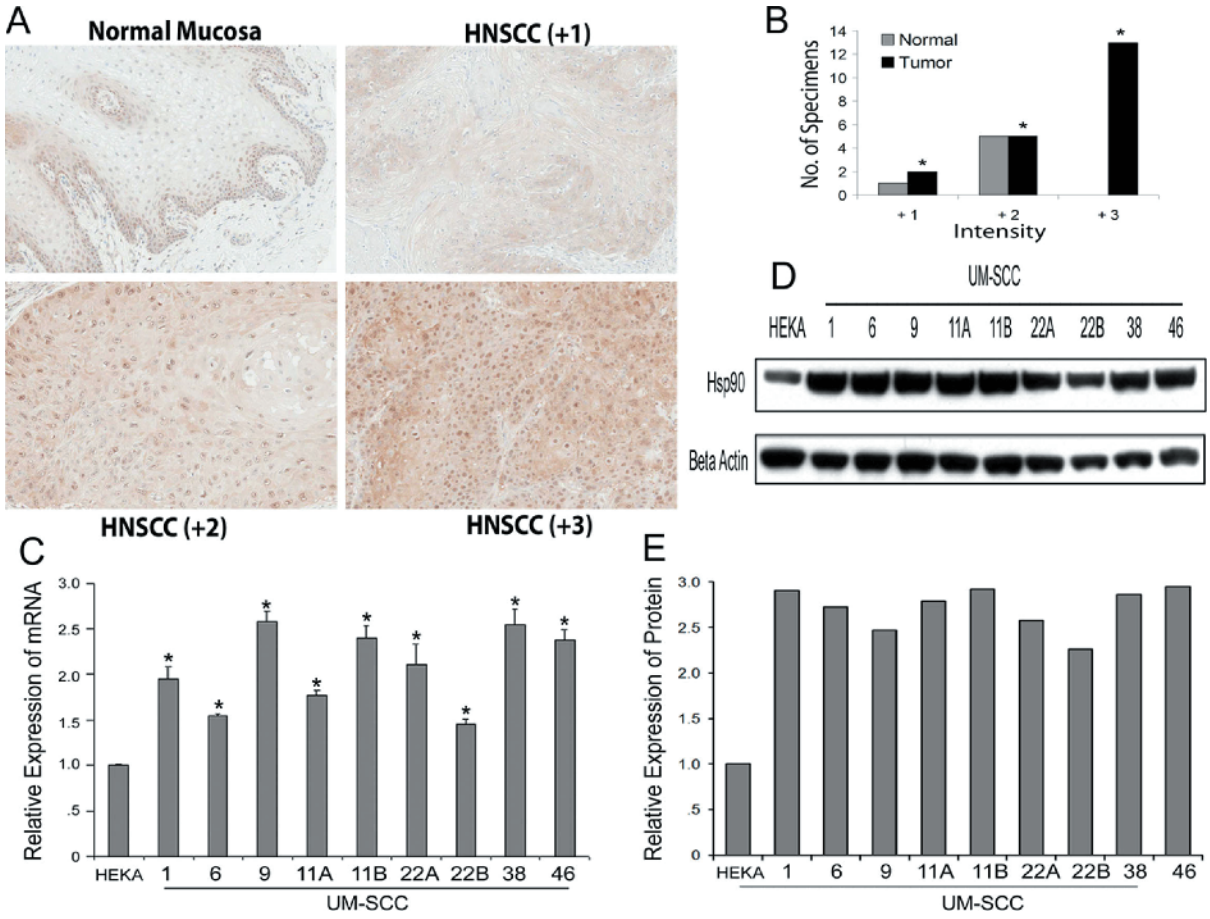

Figure W1. HSP90 is overexpressed in human HNSCC and in UMSCC cell lines. (A) Representative tissue sections of immunohistochemical staining patterns for total HSP90 protein expression in normal human oral squamous epithelium and in three representative HNSCC tumor specimens exhibiting low (+1), moderate (+2), and high (+3) staining intensity patterns. Original magnification, ×200. (B) Comparison of staining intensity score distributions between normal and tumor specimens shows that distribution of higher HSP90 staining intensity is greater in tumors compared to normal specimens, Fisher's exact test ($P = .01$). (C) HSP90 mRNA expression in UMSCC cell lines. Total RNA was isolated from HEKA cells (normal proliferating human epithelial keratinocytes) and nine UMSCC cell lines. HSP90 mRNA expression was determined by real-time RT-PCR. *$P < .05$ denotes statistical significance by Student's *t* test. (D, E) Western blot and densitometry analysis of HSP90 protein expression in UMSCC cell lines compared to HEKA controls.

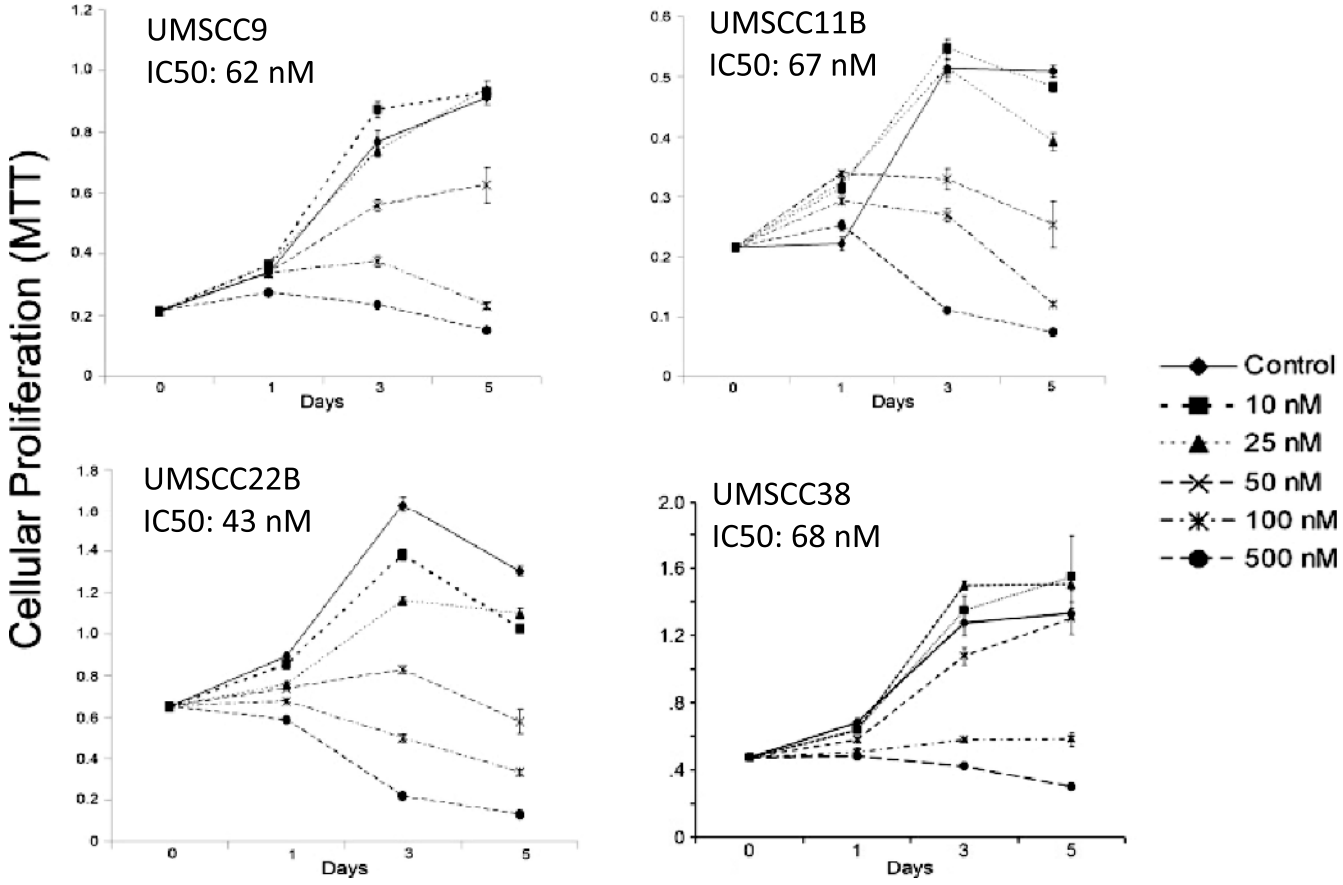

Figure W2. *In vitro* effect of SNX2112 on cellular proliferation in UMSCC-9, -11B, -22B, and -38 cell lines. Cellular proliferation was measured by MTT-based colorimetric assay in UMSCC-9, -11B, -22B, and -38 cells after 1, 3, and 5 days of drug treatment. Cell lines were treated with five drug doses with increasing concentrations, leading to progressive inhibition of cellular proliferation.

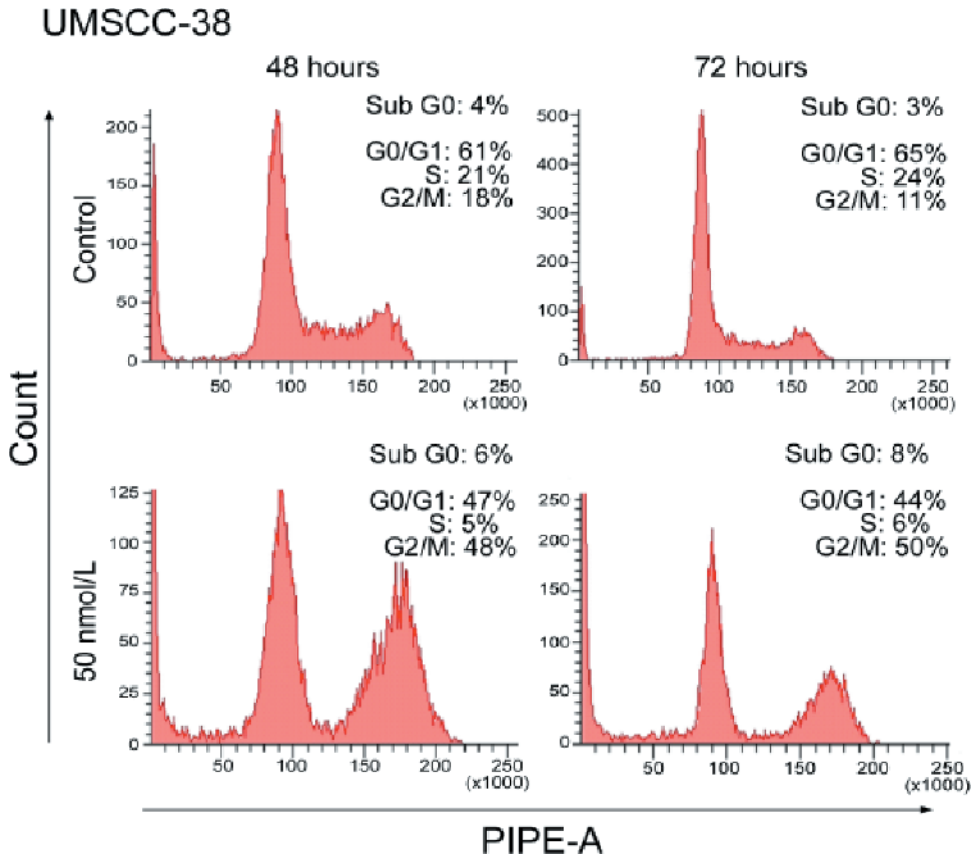

Figure W3. SNX2112 induces cell cycle arrest in UMSCC-38 cells *in vitro*. Flow cytometric cell cycle analysis was performed using propidium iodide DNA staining of UMSCC-38 cells following 48 and 72 hours of treatment with 50 nM SNX2112. Drug treatment for both 48 and 72 hours decreased the number of cells in the G_0/G_1 and S phases and induced a substantial accumulation of cells in the G_2/M phase, as well as a more modest increase in the number of apoptotic cells in the sub-G_0 phase.

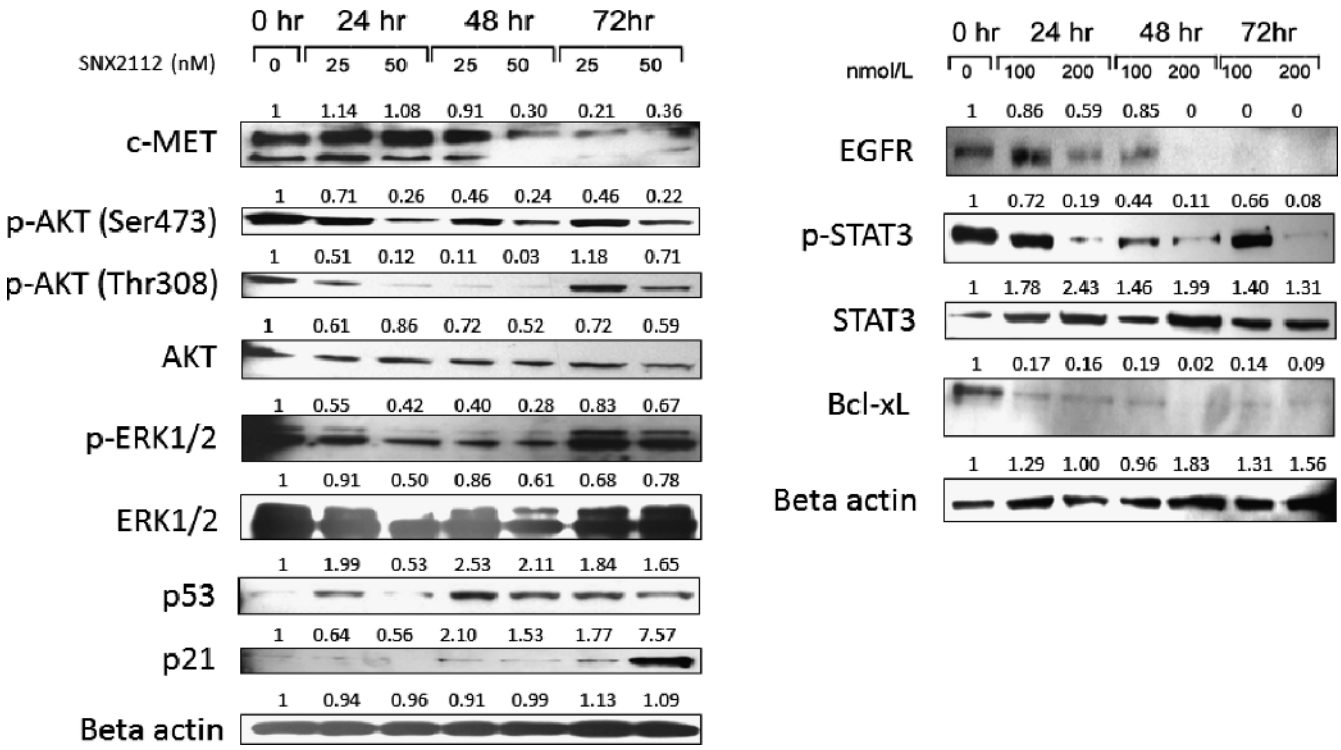

Figure W4. Effects of SNX2112 on oncogenic HSP90 clients or dependent proteins in UMSCC-38. Western blot analysis of whole-cell lysates from mtTP53 UMSCC-38 cell line treated with 25 or 50 nM SNX2112 (left panel) or 100 or 200 nM SNX2112 (right panel) for 24, 48, and 72 hours. Clients examined demonstrate sensitivity to lower or higher concentrations with enhanced p53 and target p21 expression similar to those observed for UMSCC-1.

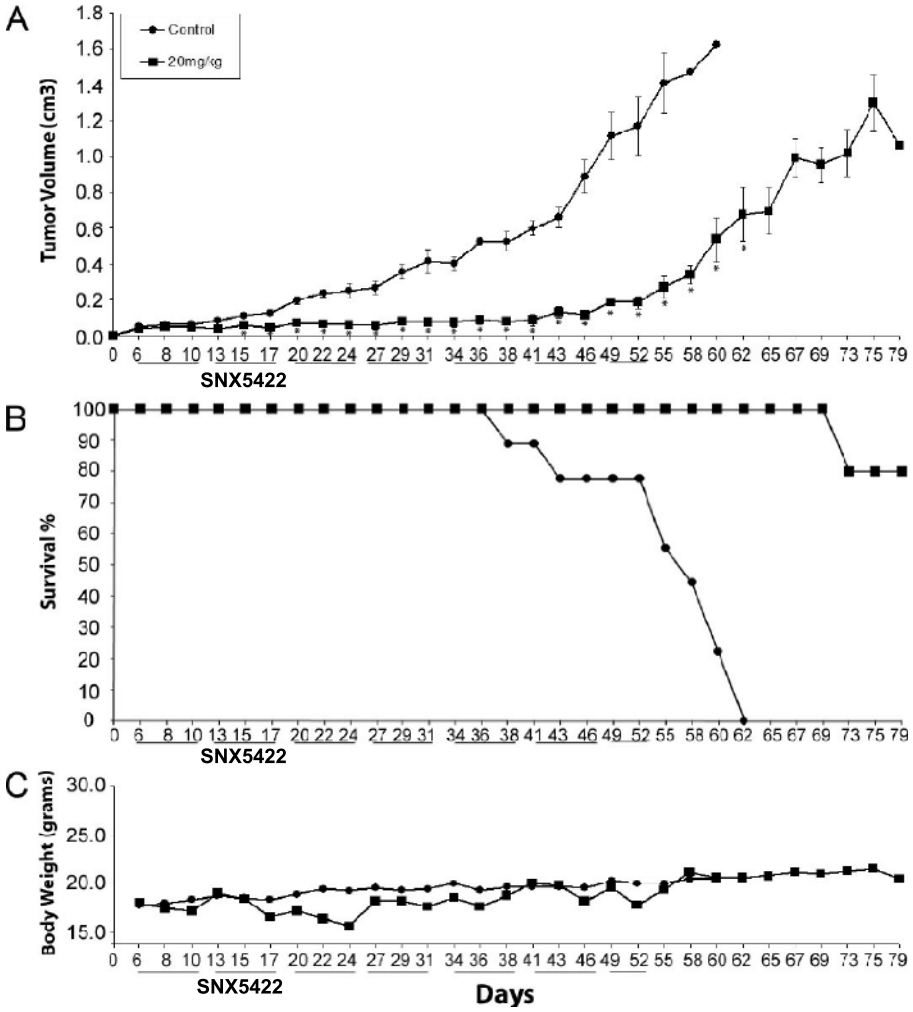

Figure W5. Effect of long-term SNX5422 treatment on tumor growth of UMSCC-1 *in vivo*. Placebo-controlled study of treatment with 20 mg/kg prodrug SNX5422 for 6.5 weeks revealed inhibition of tumor growth and an overall survival benefit. Comparison of (A) tumor growth, (B) survival curves, and (C) body weight between control and treated animals. *$P < .05$ indicates statistical difference between control and 20 mg/kg treated group (Student's *t* test).